IFA - 95/42 Sept. 1995

AARHUS-ASTRO-1995-22 ISSN 0906-3870

EXTINCTION IN NGC 628 AND NGC 2403 DERIVED FROM PASCHEN AND BALMER LINES

L. Petersen and P. Gammelgaard

Inst. of Physics and Astronomy
University of Aarhus
DK-8000 Aarhus C
Denmark

To appear in Astronomy and Astrophysics

A&A manuscript no.
(will be inserted by hand later)

Your thesaurus codes are:
3(11.19.2;11.09.3;09.04.1;09.08.1)

ASTRONOMY
AND
ASTROPHYSICS
4.9.1995

Extinction in NGC 628 and NGC 2403 derived from Paschen and Balmer lines *

L. Petersen and P. Gammelgaard

Institut for Fysik og Astronomi, Aarhus Universitet, Ny Munkegade, DK-8000 Århus C, Denmark

Received ; Accepted

Abstract. Long-slit spectrophotometry obtained simultaneously in the spectral ranges $\lambda\lambda$3950–4900 Å and 8000–10500 Å is presented for a number of giant extragalactic H II regions (GEHRs) in the spiral galaxies NGC 628 and NGC 2403. These ranges include lines from the Balmer and Paschen series of hydrogen separated by a wide wavelength interval. The Paschen and Balmer lines with special emphasis on the corresponding multiplet lines Pδ/Hϵ are used to examine the dust extinction towards the GEHRs in these galaxies. We find good internal consistency for the observed/predicted line ratios used for derivation of the visual extinction, A_V.

Our results for A_V are in general larger than previously published values based on the Hα/Hβ ratio with the GEHRs in NGC 628 exhibiting the largest extinction.

Key words: galaxies: spiral – galaxies: ISM – dust, extinction – H II regions

1. Introduction

Studies of both Galactic and extragalactic H II regions rely on correction for the effect of dust on the observed spectral energy distribution. Interstellar extinction remains one of the most serious sources of systematic error in visible and UV measurements of H II regions and star forming regions in galaxies. Knowledge of the dust extinction and its spatial distribution is consequently important for our understanding of the physical state in such dusty objects.

Usually, the total visual extinction, A_V, is determined by comparison of the emergent flux ratio at two distinct wavelengths for which the intrinsic ratio is known, but also broad-band optical and near-IR colours, the FIR and submillimetre continuum, the 10 μm absorption feature, etc. have been used. For a comparison of the various methods for the center of M82 see Götz et al. (1990), Puxley (1991), McLeod et al. (1993).

In the optical regime a number of spectral lines from recombination of hydrogen are available for extinction determination. Most often Hα and Hβ have been used due to their large strengths and positions at wavelengths spectroscopically easily accessible. On the other hand it is clearly an advantage to use line pairs, which are separated by a wide wavelength interval over which the extinction has a large effect. For example recently Puxley & Brand (1994) used the near-IR Paschen and Brackett lines together with existing data on optical lines for determination of the dust extinction in two starburst galaxies. In addition the intrinsic ratio of any two lines from the Balmer series relies on a recombination line model (cf. Osterbrock, 1989) and the knowledge of the electron temperature and density (T_e, n_e), since the transitions originate at different levels in the hydrogen atom.

To benefit both by a wide wavelength interval and by minimized dependency on recombination line model calculations it has long been proposed (cf. Greve et al. 1994 and references therein) to use corresponding multiplet lines from the Paschen and Balmer series, Pn/Hn, originating from the same upper atomic level, as ideal extinction indicator, since the relative strengths depend primarily on the transition probabilities (Greve et al. 1989, 1994) and only slightly on the excitation conditions (Osterbrock 1989).

Many of the Paschen and Balmer lines can be observed with modern CCD detectors provided a correct elimination of the strong OH sky emission lines at $\lambda > 7000$ Å is carried out. Thus, we aim at measuring the flux from the blue Balmer lines and as many Paschen lines as possible *simultaneously* with the *same* telescope and through the *same* aperture, with special emphasis on the corresponding multiplet lines to study the dust extinction of giant extragalactic H II regions.

Here we present two-channel blue and near-IR spectroscopic observations of a number of H II regions in NGC 628 and NGC 2403 as part of a larger study of the dust extinction of GEHRs in spiral galaxies. The blue wave-

Send offprint requests to: larsp@obs.aau.dk

* Based on observations collected at the Nordic Optical Telescope, La Palma, Spain

length region covers the Balmer lines Hϵ–Hβ, while the near-IR region contains the Paschen lines Pδ–P14 making the Pδ/Hϵ line ratio available.

2. Observations

Observations were carried out at the 2.5-m Nordic Optical Telescope, La Palma, Spain with the long-slit Århus-Tromsø Low Dispersion Spectrograph (LDS) in January 1994 supplemented with observations from July 1994.

The spectrograph consists of two channels optimized for the red and blue part of the spectrum with a dispersion of 7.5 Å/pixel and 2.0 Å/pixel, respectively, and equipped with a P8603 and a TK512 CCD. The length of the slit is $\sim 4'$ and when possible the spectrograph was rotated to a position angle allowing two H II regions to be observed simultaneously. A journal of the observations is presented in Table 1.

Exposures of P14–Pδ and Hϵ–Hβ were taken simultaneously in the two channels ensuring that all lines are influenced by the same atmospheric conditions in order to obtain very precise relative spectrophotometry.

The spectrophotometric standard stars from Oke (1983) indicated in Table 1, which all have the flux distribution given out to 1.2 μm, were observed several times during the night at airmasses encompassing those of the objects to enable flux calibration and correction for the atmospheric H_2O absorption band at $\lambda\lambda$8900–9800 Å by means of the method outlined by Osterbrock et al. (1990).

2.1. Data reduction

The CCD frames were reduced with standard IRAF packages including flat fielding, illumination correction and atmospheric extinction correction appropriate for La Palma. Calibration spectra of Cd/Hg and Cs spectral lamps were taken just prior to and right after the observations for wavelength calibration. Rectification of the 2-dimensional frames were carried out by introducing a special mask with a series of equally spaced holes parallel to the slit in the light beam. Due to the different physical sizes of the CCD's this produces 5 and 7 parallel spectra in the blue and red channel each separated by 44.″4, that are used for mapping the spatial direction along the slit.

Since the exposure times were long, generally 20 min to accomplish a proper sampling of the object spectra, most of the frames are hampered by cosmic ray hits. These events were rejected by applying the IMSYS routine *cosmic* (Thomsen, priv.comm.) that fits polynomials at every pixel accounting properly for readout noise, gain and the spectral nature of the frame.

Careful measures were taken to make the extraction apertures match exactly in the rectified frames of the two wavelength ranges, with the lengths set to cover all pixels showing emission in each GEHR and with the widths of the apertures dictated by the slit width of 2.″2 corresponding to 4.7 pixels in the blue and 2.6 pixels in the red channel. The sky background has been sampled over a large part of the frame around the H II regions to increase S/N of the many disturbing OH sky emission lines. In Fig. 1 we present an example of the final calibrated blue and near-IR spectra. In the blue spectrum note also the broad feature at $\lambda \sim 4650$ Å assigned to Wolf-Rayet stars (Fierro et al. 1986). At P15 we tend to reach the series limit giving rise to a false continuum, which makes flux measurements unreliable.

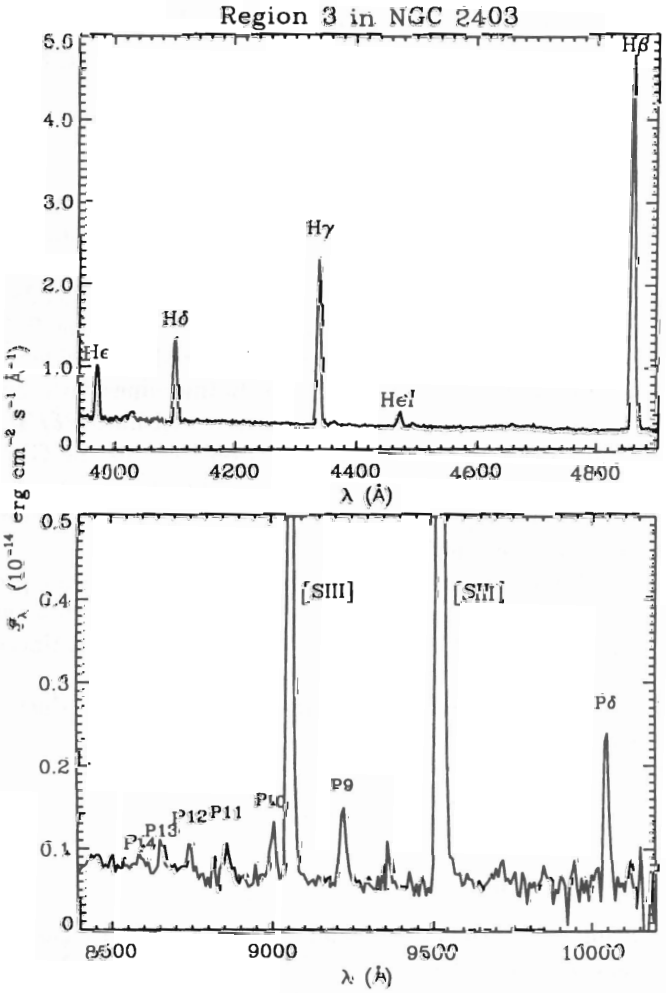

Fig. 1. a Blue spectrum of H II region 3 in NGC 2403 showing four strong Balmer emission lines. b Near-IR spectrum of the same region. The faint Paschen lines down to P14 are clearly identified

2.2. Flux determination

The flux in the individual spectral lines were measured both by simply summing under the line and by fitting a Gaussian profile to the line and integrating under this profile. The two methods give values which differ only slightly. We have deblended the Hϵ emission line from the [NeIII] line at 3967.46 Å by fitting two Gaussians.

Table 1. Journal of observations with the numbering of H II regions following Fierro et al. (1986) and Belley & Roy (1992)

Date	Object	$\Delta\alpha$[a] (″)	$\Delta\delta$[a] (″)	Aperture (″)	Total exp. (s)	Standard stars
1994 Jan 2	NGC 2403 Reg. 1	+10	+32	10.0 × 2.2	3600	HD 19445, HD 84937
1994 Jan 2	NGC 2403 Reg. 2	−45	+55	5.8 × 2.2	1200	HD 19445, HD 84937
1994 Jan 2	NGC 2403 Reg. 3	+96	+35	26.7 × 2.2	3600	HD 19445, HD 84937
1994 Jan 2	NGC 2403 Reg. 4	−186	+45	8.3 × 2.2	1200	HD 19445, HD 84937
1994 Jul 31	NGC 628 Reg. 27	+46	+49	7.5 × 2.2	3600	BD 174708
1994 Aug 1	NGC 628 Reg. 79	−56	−110	7.5 × 2.2	6000	BD 174708
1994 Jan 1	NGC 628 Reg. 83	−48	−152	11.2 × 2.2	3000	HD 19445, HD 84937

[a] Offsets are from nucleus of galaxy east and north being positive

The measured line fluxes for all Paschen and Balmer lines detected in the 7 regions (3 in NGC 628 and 4 in NGC 2403) are given in Table 2 as well as parameters necessary for calculating A_V. The accuracy of the fluxes is $\approx$ 5% in the blue region, except for Hϵ where the deblending may be uncertain by $\sim$ 20%, judged from the rms scatter of the sensitivity functions and from a comparison with published data for regions in common with McCall et al. (1985) and Fierro et al. (1986). In the near-IR wavelength region the sky subtraction is much more critical, leading to accuracies of 10-20 %. In column (3) the normalized extinction function is given and in column (4) we list the intrinsic line ratios for case B recombination (standard values $T_e = 10^4$ K and $n_e = 10^2$ cm^{-3}).

The values of $\log \mathcal{F}(H\beta)$ agree well with those found by McCall et al. (1985) and Fierro et al. (1986), but these absolute numbers are naturally very sensitive to the size of the aperture used and the exact position of the slit.

3. Determination of the visual extinction

The total extinction is derived from comparison of the observed emission line flux ratios R_o, and the flux ratios R_p predicted in the absence of extinction.

3.1. Predicted line ratios and extinction function

Theoretical line ratios for case B recombination of hydrogen have been calculated by Hummer & Storey (1987) for a total of 48 levels taking full account of collisional effects. Due to the l-degeneracy of the energy levels in the hydrogen atom the line ratios, even for corresponding multiplet lines, depend weakly on excitation conditions, T_e, n_e.

GEHRs have low densities with $n_e \sim 10$ to 100 cm^{-3} (McCall et al. 1985) and for $T_e = 7500$–12500 K the variation of R_p is very small, e.g. 0.34–0.36 for Pδ/Hϵ. Values for T_e and n_e determined by Fierro et al. (1986) for the regions in NGC 2403 confirm that they are within these intervals.

We used typical values of 100 cm^{-3} and 10000 K, and as pointed out by Greve et al. (1994) neglecting the weak dependence introduces an uncertainty, over the wide wavelength interval used, that is smaller than the expected overall observational errors.

Assuming an (effective) uniform absorbing foreground screen, A_V can be calculated from the observed and predicted ratios of two emission lines at λ_1 and λ_2 as

$$A_V = \frac{2.5\, R_V\, \log\left(\frac{R_o}{R_p}\right)}{F(\lambda_2) - F(\lambda_1)} \tag{1}$$

where $F(\lambda) = (A_\lambda - A_V)/(A_B - A_V)$ is the normalized extinction curve (Savage & Mathis 1979; Scheffler & Elsässer 1988) and $R_V = A_V/E_{B-V}$. The extinction function can also be expressed in terms of A_λ/A_V, in that case Eq. (1) transforms into

$$A_V = \frac{2.5 \log\left(\frac{R_o}{R_p}\right)}{A_{\lambda_2}/A_V - A_{\lambda_1}/A_V}. \tag{2}$$

Here we shall use Eq. (2) adopting the average extinction law as derived from stellar photometry by Cardelli et al. (1989) in the form of

$$A_\lambda/A_V = a(\lambda) + b(\lambda)/R_V \tag{3}$$

with $a(\lambda)$ and $b(\lambda)$ given as polynomials or power laws.

Studies of the extinction in the LMC (Koornneef 1982; Howarth 1983) and the SMC (Prévot 1984; Bouchet et al. 1985) reveal extinction laws that look similar to the average Galactic curve for the optical and near-IR regions, confirming the assumption that the Galactic extinction function can be used for these wavelengths even in galaxies of different chemical compositions.

When observing extended regions the actual geometrical distribution, e.g. clumpiness or patchiness, of the dust and the scattering of in particular blue photons back into the line of sight by dust situated close to the emitting source can make the effective extinction curve more

Table 2. Observed line fluxes (normalized at $\mathcal{F}(\mathrm{H}\beta) = 1$)

				$\left(\frac{\mathcal{F}(\lambda)}{\mathcal{F}(\mathrm{H}\beta)}\right)_o$						
				NGC 628			NGC 2403			
λ	ID	$\frac{A_\lambda}{A_V}$ ($R_V = 3.1$)	$\left(\frac{I(\lambda)}{I(\mathrm{H}\beta)}\right)_p$	Reg. 27	Reg. 79	Reg. 83	Reg. 1	Reg. 2[b]	Reg. 3	Reg. 4
3970	Hϵ	1.474	0.159	0.131	0.093	0.101	0.121	0.119	0.113	0.103
4102	Hδ	1.431	0.259	0.247	0.211	0.195	0.208	0.234	0.209	0.181
4340	Hγ	1.346	0.468	0.390	0.391	0.391	0.406	0.434	0.416	0.410
4861	Hβ	1.164	1.000	1.000	1.000	1.000	1.000	1.000	1.000	1.000
8598	P14	0.519	0.00666						0.013	
8665	P13	0.512	0.00832						0.016	
8750	P12	0.503	0.0106				0.018		0.019	
8863	P11	0.491	0.0138	0.044			0.022		0.027	
9015	P10	0.478	0.0184	0.072	0.060		0.032	0.031	0.038	0.039
9229	P9	0.460	0.0254	0.083	0.073	0.055	0.042	0.039	0.056	0.063
10049	Pδ	0.401	0.0555	0.215	0.188	0.180	0.098	0.118	0.112	0.195
log $\mathcal{F}(\mathrm{H}\beta)$[a]				-13.54	-13.66	-13.32	-13.00	-12.82	-12.43	-12.93

[a] In units of erg cm^{-2} s^{-1}

[b] Corrected for underlying Balmer absorption, see text

grey than the uniform interstellar extinction which is used when dealing with point sources, as discussed by Caplan & Deharveng (1986), Witt et al. (1992) and Calzetti et al. (1994).

It is therefore not straightforward to apply the extinction function derived from stellar observations to extended regions. Consequently, we will analyse the data with the standard extinction function with $R_V = 3.1$ valid for the diffuse interstellar medium (Cardelli et al. 1989) for easy comparison with values from the literature based on Hα/Hβ, and in addition apply a much greyer curve described by a Cardelli et al. curve with $R_V = 6$ to one of the H II regions as an illustrating example. Changing the value of R_V will only influence the lines in the blue part of the spectrum, since the extinction function is independent of R_V for $\lambda > 7000$ Å (Cardelli et al. 1989).

3.2. Results

A_V can be derived from Eq. (2) for any pair of the observed hydrogen emission lines in the GEHRs, but we shall here concentrate on the corresponding multiplet lines Pδ/Hϵ and a weighted fit of the entire data set covering the wide wavelength interval observed.

The stellar continuum rises towards short wavelengths in the blue spectral region and thereby increases the effect of the underlying Balmer absorption on the emission lines, which leads to overestimation of the extinction. Of the H II regions observed here only region 2 in NGC 2403 seems to be affected significantly by underlying Balmer absorption (cf. Fierro et al. 1986) and the line ratios have been corrected by adopting the average absorption equivalent width of 1.9 Å from McCall et al. (1985) for the lines Hβ–Hϵ. That the rest of the observed H II regions are unaffected or only suffer from absorption to a very small degree is based on three considerations. They all have $EW(\mathrm{H}\beta) \geq 70$ Å, a limit below which the underlying absorption lines steepen the emission decrement significantly (McCall et al. 1985). None of them show a strong rise of the continuum in their spectra (cf. Fig. 1), and nor do any of them display a systematic deviation blueward of Hβ below the linear relation used for extinction determination (Fig. 2).

The derived value of A_V based on the Pδ/Hϵ corresponding multiplet lines and the standard extinction function is given as the first entry in Table 3. For all other line pairs A_V could be calculated from the measured line fluxes in Table 2 using Eq. (2), but instead an average value of the visual extinction based on all observed lines was obtained from a weighted fit of the line fluxes. In Fig. 2 the observed line fluxes measured in H II region 3 in NGC 2403 have been plotted relative to Hβ in the form $2.5 \log(R_o/R_p)$ as a function of A_λ/A_V for $R_V = 3.1$. When displayed in this way the line ratios show, according to Eq. (2), a linear relation with a slope equal to $-A_V$ and illustrate the advantage of using a wide wavelength interval. The dashed line represents a weighted least-square straight line fit to the data points with error bars indicating estimated observational uncertainties.

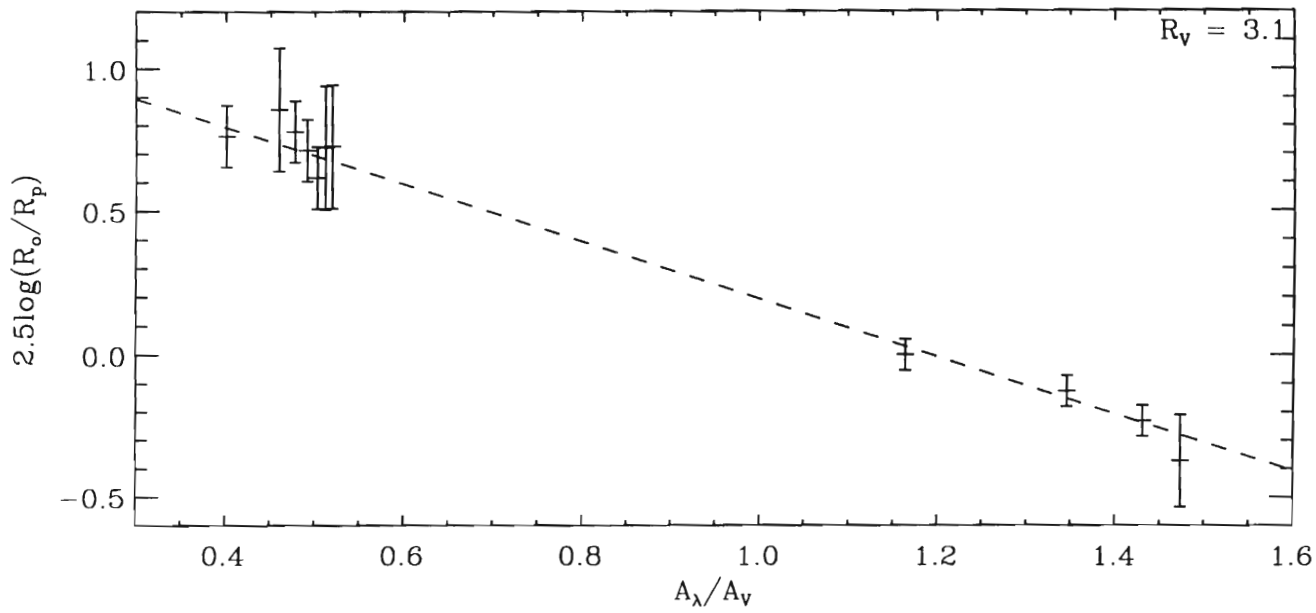

Fig. 2. Observed line ratios for the Paschen and Balmer lines of H II region 3 in NGC 2403. The dashed line represents a least-square fit with a gradient equal to $-A_V$

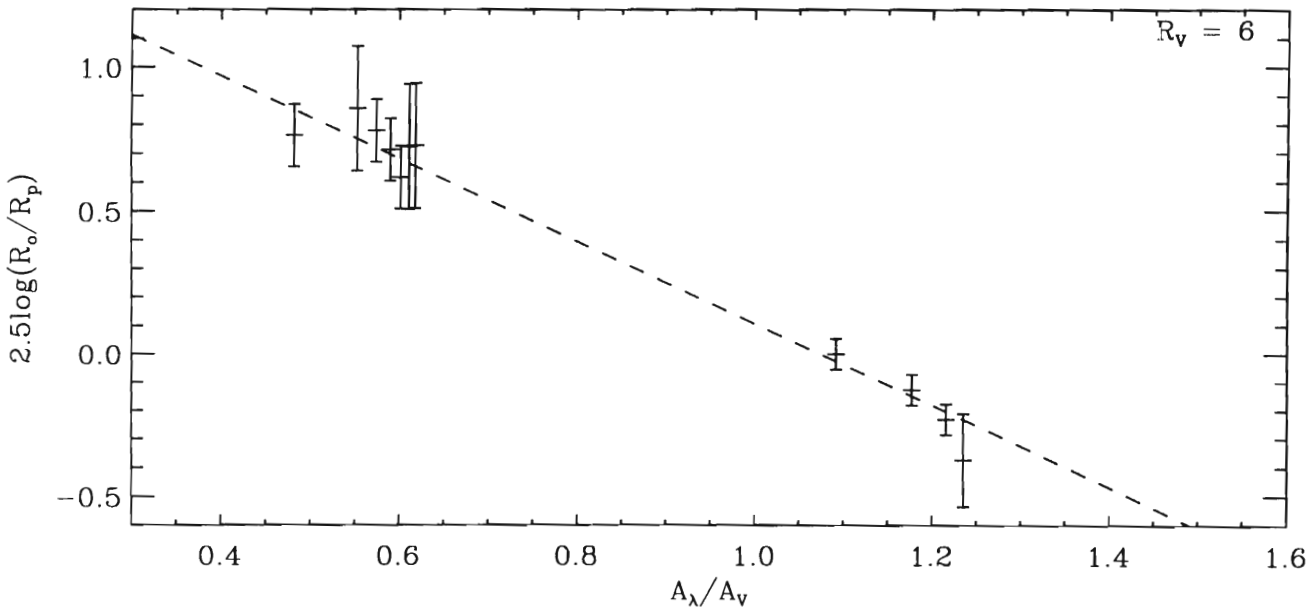

Fig. 3. Same as Fig. 2 but for an effective extinction function with $R_V = 6$. A_λ/A_V is now closer to unity for all the emission lines and the slope of the dashed line must therefore be larger to match the observed line fluxes

The effect of a greyer effective extinction curve is illustrated in Fig. 3 where the observed line fluxes are plotted versus A_λ/A_V for $R_V = 6$. In this case a higher value of A_V is required to fit the data points. The two dashed lines fit the data almost equally well, with $A_V = 1.00 \pm 0.03$ in Fig. 2 and $A_V = 1.44 \pm 0.06$ in Fig. 3 and we cannot significantly distinguish between the two effective extinction curves from these data. With the inclusion of near-IR lines at longer wavelengths, however, discrimination among different physical dust distribution can be made as shown by Puxley & Brand (1994).

Similar fits have been applied to the other H II regions and the calculated values for A_V corresponding to $R_V =$

Table 3. Visual extinction A_V (mag) for the 7 observed extragalactic H II regions. All numbers in this table are derived with $R_V = 3.1$

	NGC 628			NGC 2403			
	27	79	83	1	2	3	4
A_V, Pδ/Hϵ	1.57	1.78	1.65	0.84	1.05	1.06	1.59
A_V, linear fit	1.61 ± 0.17	1.58 ± 0.11	1.47 ± 0.10	0.83 ± 0.02	0.81 ± 0.09	1.00 ± 0.03	1.45 ± 0.10
A_V, Hα/Hβ[a]	2.12 ± 0.28	0.99 ± 0.28	1.03 ± 0.14	0.71 ± 0.14			
A_V, Hα/Hβ[b]				0.77 ± 0.22	i 0.55 ± 0.22	0.87 ± 0.22	0.77 ± 0.22
A_g	0.09	0.09	0.09	0.12	0.12	0.12	0.12

[a] From McCall et al. (1985)
[b] Derived from Fierro et al. (1986)

3.1 and their associated 1σ deviations are listed in Table 3.

Results for the corresponding multiplets lines and the linear fit are in agreement, but there is a tendency to larger values of A_V derived from the Pδ/Hϵ line pair. This could be due to an underestimation of the Hϵ line flux in the deblending procedure. For comparison purposes we have listed previously determined A_V values based on Hα/Hβ in Table 3.

Except for the high value of H II region 27 in NGC 628 found by McCall et al. (1985) the results for A_V derived in this study are somewhat larger than the previously published results based on Balmer emission lines.

The Galactic foreground extinction A_V(Gal) affects the emission lines at the observed redshifted wavelengths. The contribution from Galactic extinction to the total visual extinction as calculated from Eq. (2) therefore takes the form

$$A_V(\mathrm{Gal}) = A_g \frac{A_{\lambda_{2,o}}/A_V - A_{\lambda_{1,o}}/A_V}{A_{\lambda_2}/A_V - A_{\lambda_1}/A_V} \quad (4)$$

where A_{λ_o}/A_V is the extinction function at the observed wavelengths. For the low redshifts of NGC 2403, $v_r = 107 \pm 32$ km/s (essentially no redshift) and NGC 628, $v_r = 632 \pm 23$km/s (de Vaucouleurs et al. 1991), the ratio is equal to unity, and the extragalactic extinction component can be derived simply by subtracting the values of A_g given by de Vaucouleurs et al. (1991) from A_V. This has not been done for the values given in Table 3.

For NGC 628 the derived extragalactic extinctions are in the interval 1.4–1.6, while for NGC 2403 we derive A_V (Exgal) = 0.7–1.3. Again this is in good overall agreement with McCall et al. (1985) who also found the former to exhibit the larger extinction but with larger variations from region to region, although they used larger values for the Galactic extinction.

4. Conclusion

Optical and near-IR spectrophotometry of Paschen and Balmer emission lines obtained simultaneously through the same aperture has been used to examine to dust extinction of giant extragalactic H II regions in the spiral galaxies NGC 628 and NGC 2403. The Paschen and Balmer lines have wider wavelength separations than the strong Balmer lines commonly used for extinction determination. Consequently, A_V can be determined from these weak lines with the same uncertainty as for the easily observable strong Balmer lines in spite of larger observational errors, since the denominator of Eq. (2) will be ~ 3 times larger for the Paschen-Balmer combinations as compared to Hα/Hβ.

We consider Pδ/Hϵ as the best extinction indicator based on a single line pair, since this ratio has the longest baseline and the emission lines originate from a common upper level, although the deblending of Hϵ can be uncertain. In addition, Pδ fortuitously is not affected by atmospheric H_2O absorption bands or OH sky emission lines.

We thus have demonstrated the feasibility of observing Paschen-Balmer line pairs in GEHRs and of the reduction techniques for extraction of the Paschen lines from the crowded sky background in the near-IR region. The use of simultaneous exposures of optical and near-IR spectra forming a long baseline for extinction determination has lead to accurate values of the visual extinction of giant extragalactic H II regions. With improving detector sensitivity this method could be extended to more regions and also include the favourable corresponding multiplet lines Pγ/Hδ, which has successfully been applied to the Galactic Orion Nebula (Greve et al. 1994; Osterbrock et al. 1992; Petersen 1994).

Acknowledgements. This work was partially supported by The Danish Board for Astronomical Research and University of Aarhus Research Foundation. We appreciated the comments of the referee Dr. J. Caplan.

References

Belley J., Roy J.-R., 1992, ApJS 78, 61
Bouchet P., Lequeux J., Maurice E., Prevot L., Prevot-Burnichon M.L., 1985, A&A 149, 330
Calzetti D., Kinney A.L., Storchi-Bergmann T., 1994, ApJ 429, 582
Caplan J., Deharveng L., 1986, A&A 155, 297
Cardelli J.A., Clayton G.C., Mathis J.S., 1989, ApJ 345, 245
de Vaucouleurs G., de Vaucouleurs A., Corwin H.G. et al., 1991, Third Reference Catalogue of Bright Galaxies, Springer-Verlag, New York.
Fierro J., Torres-Peimbert S., Peimbert M., 1986, PASP 98, 1032
Götz M., McKeith C.D., Downes D., Greve A., 1990, A&A 240, 52
Greve A., McKeith C.D., Barnett E.W., Götz M., 1989, A&A 215, 113
Greve A., Castles J., McKeith C.D., 1994, A&A 284, 919
Howarth I.D., 1983, MNRAS 203, 301
Hummer D.G., Storey P.J., 1987, MNRAS 224, 801
Koornneef J., 1982, A&A 107, 247
McCall M.L., Rybski P.M., Shields G.A., 1985, ApJS 57, 1
McLeod K.K., Rieke G.H., Rieke M.J., Kelly D.M., 1993, ApJ 412, 111
Oke J.B., Gunn J.E., 1983, ApJ 266, 713
Osterbrock D.E., 1989, Astrophysics of Gaseous Nebulae and Active Galactic Nuclei, University Science Books, California.
Osterbrock D.E., Shaw R.A., Veilleux S., 1990, ApJ 352, 561
Osterbrock D.E., Tran H.D., Veilleux S., 1992, ApJ 389, 305
Petersen L., 1994, M.Sc. thesis
Prévot M.L., Lequeux J., Maurice E., Prévot L., Rocca-Volmerange B., 1984, A&A 132, 289
Puxley P.J., 1991, MNRAS 249, 11P
Puxley P.J., Brand P.W.J.L., 1994, MNRAS 266, 431
Savage B.D., Mathis J.S., 1979, ARA&A 17, 73
Scheffler H., Elsässer H., 1988, Physics of the Galaxy and Interstellar Matter, Springer-Verlag, Germany
Witt A.N., Thronson Jr. H.A., Capuano Jr. J.M., 1992, ApJ 393, 611

This article was processed by the author using Springer-Verlag LaTeX A&A style file *L-AA* version 3.